nature climate change

Analysis

https://doi.org/10.1038/s41558-025-02362-6

Consequential differences in satellite-era sea surface temperature trends across datasets

Received: 20 November 2024

Accepted: 23 May 2025

Published online: 11 July 2025

Check for updates

S. Menemenlis [1] ✉, G. A. Vecchi [2,3], Wenchang Yang [2], S. Fueglistaler [1,2] & S. P. Raghuraman [4]

Global surface temperatures since the 1980s, when near-global satellite-based sea surface temperature (SST) measurements became available, are presumed to be well known. Satellite-era warming trends in four commonly used global (land and ocean) temperature reconstructions agree closely, yet whether SST datasets also agree is unclear. Here we show that trends in four widely used SST datasets show first-order differences, with 1982–2024 60° S to 60° N trends ranging from 0.108 to 0.184 °C per decade. These large discrepancies are perplexing given the agreement between global temperature datasets and the fact that 70% of the surface of the Earth is covered by ocean, but are legible upon recognizing that global temperature datasets use two SST fields whose trends agree more closely than those of the four SST datasets. Considering the trend uncertainty across SST datasets widens the range of plausible global temperature trends and impacts interpretations of recent record global temperatures, with implications for observational and model-based climate studies.

Although estimates of global temperatures based on direct observations are available dating back to the mid-nineteenth century, such reconstructions are assumed to be best known in recent decades. The quantity and coverage of in situ surface marine observations from ships, drifting and moored buoys and fixed observing stations have increased over time, and are collected in the international comprehensive ocean–atmosphere dataset (ICOADS)[1]. Near-global remote sensing of sea surface temperatures (SSTs) from satellites using infrared measurements began in the early 1980s and microwave SST measurements began in late 1997.

Reconstructing global SSTs, whether from a combination of in situ and remote observations or from in situ observations only, requires combining heterogeneous and spatiotemporally incomplete data. Different sampling methods produce different measurement patterns in space and time, and may define 'surface' temperature at different depths, from several metres below the surface for ship intake measurements to upper micrometres of the ocean surface for infrared satellites. Each observation carries uncertainty and may need to be corrected for known biases. Such adjustments may have notable effects on decadal-scale global temperature trends[2].

A handful of institutions produce regularly updated, spatially complete, global SST reconstructions for public access. These datasets, with version numbers current at the time of writing, are the sea ice and SST of the Hadley Centre (HadISST1)[3] from the UK Met Office; the extended reconstructed sea surface temperature version 5 (ERSST v.5)[4] and daily optimum interpolation sea surface temperature version 2.1 (OISST v.2.1)[5] from the US National Oceanic and Atmospheric Administration (NOAA); and the centennial in situ observation based estimates of the variability of SST and marine meteorological variables version 2 (COBE2)[6] from the Japan Meteorological Agency (JMA). These four reconstructions use much of the same observational data, but use different techniques to correct for measurement biases, homogenize and interpolate SST data, estimate SSTs in areas with sea ice and estimate uncertainties (Methods). ERSST v.5, unlike the other three datasets, uses only in situ observations for SST reconstruction.

In addition, a few global surface temperature products, which combine SSTs with reconstructions of near-surface land temperature, are regularly updated and made available for public use. These products, with current version numbers, are the Goddard Institute for Space

[1]Program in Atmospheric & Oceanic Sciences, Princeton University, Princeton, NJ, USA. [2]Department of Geosciences, Princeton University, Princeton, NJ, USA. [3]High Meadows Environmental Institute, Princeton University, Princeton, NJ, USA. [4]Department of Climate, Meteorology & Atmospheric Sciences, University of Illinois Urbana-Champaign, Urbana, IL, USA. ✉e-mail: smenemenlis@princeton.edu

https://doi.org/10.1038/s41558-025-02362-6

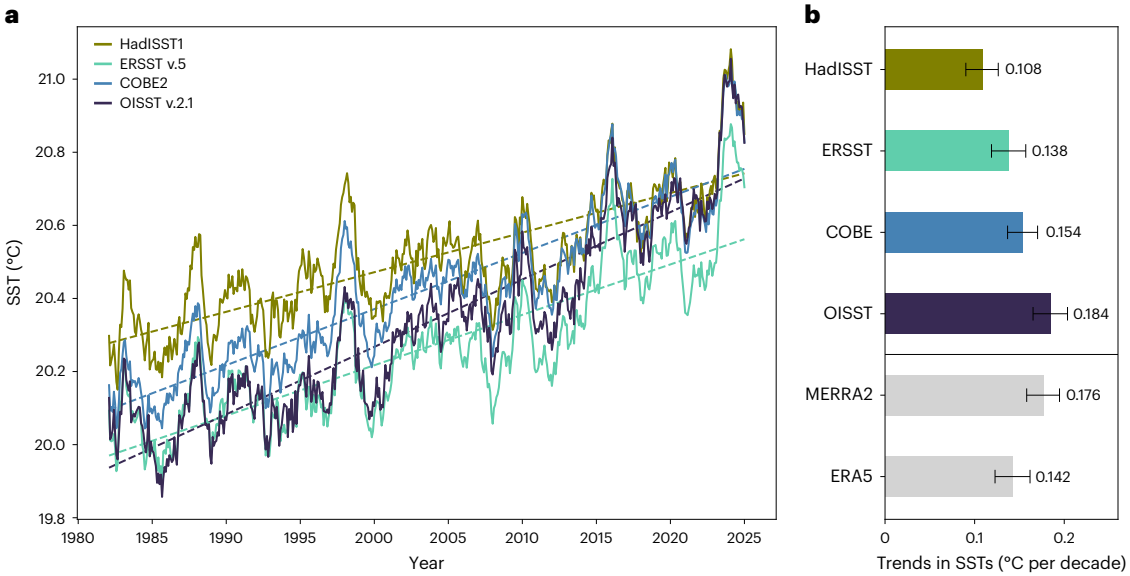

Fig. 1 | Differences in satellite-era SST trends. a, Time series of deseasonalized monthly average SSTs (°C) between 60° S and 60° N. Dashed lines show the linear trend between 1982 and 2024. HadISST1, ERSST v.5, COBE2 and OISST v.2.1 are depicted in olive, teal, blue and indigo, respectively. **b**, Trends in SSTs between 60° S and 60° N for the period 1982–2024 (n = 516 months), in °C per decade, for the same four SST datasets, plus MERRA2 and ERA5 reanalysis. Error bars represent the ±2 s.e. range based on a Newey–West standard error estimator, around the ordinary least squares regression slope.

Studies surface temperature product version 4 (GISTEMP v.4)[7,8], the UK Met Office Hadley Centre/Climatic Research Unit global surface temperature dataset version 5 (HadCRUT5)[9], the NOAA global temperature dataset version 6 (NOAAGlobalTemp v.6.0.0)[10], the Berkeley Earth global temperature dataset (Berkeley Earth)[11] from the California-based non-profit Berkeley Earth and the China global merged surface temperature version 3.0 (CMST3.0)[12].

Publicly available SST and global temperature products are an essential part of the infrastructure of climate science. They are used to monitor climate change and provide boundary conditions for climate models, as input to widely used reanalysis datasets and as references in the development of climate models. It is typical for these data to be used without explicit consideration of uncertainty and with limited comparison to other datasets.

Here we compare the aforementioned SST and global temperature products. We focus on temperature trends since the 1980s, when observational coverage is most robust, and consider average temperatures between 60° S and 60° N to avoid comparing datasets with explicitly different techniques for estimating temperatures in areas with sea ice. Our analysis demonstrates that large differences across datasets in satellite-era global SST trends exist, imply greater uncertainty in global mean temperature trends than previously apparent and impact interpretations of past and present climate.

Temperature trend uncertainty

The five publicly available global surface temperature datasets—CMST3.0, NOAAGlobalTemp v.6.0.0, Berkeley Earth, GISTEMP v.4 and HadCRUT5.0.2—exhibit very similar 60° S–60° N 1982–2024 land and ocean warming trends of 0.185, 0.189, 0.190, 0.191 and 0.192 °C decade^{-1}, respectively. Over this same area and time period, the four SST datasets—HadISST1, ERSST v.5, COBE2 and OISST v.2.1—exhibit trends of 0.108, 0.138, 0.154 and 0.184 °C decade^{-1}, respectively (Fig. 1). That is, satellite-era warming trends differ between SST datasets by up to ~70%. The differences between SST datasets cannot be explained by any single ocean region or latitude range; they are global in scale (Supplementary Figs. 1–4; the reader is also referred to these supplementary figures for further inspection of regional differences).

HadISST1, ERSST v.5, COBE2 and OISST v.2.1 drift in relation to one another at the decadal scale, despite similar spatial warming patterns (Supplementary Fig. 3) and consistent year-to-year variability. HadISST consistently records higher absolute temperatures than ERSST, with the offset between the two products narrowing slightly over the satellite era. COBE and (most prominently) OISST drift from temperatures more similar to ERSST to those more similar to HadISST, such that COBE, OISST and HadISST record similar temperature values over the last decade. It is also informative to compare SST trends from reanalysis datasets, which are used for similar applications to observational SST reconstructions. The SST trend in MERRA2 reanalysis is closest to that of OISST v.2.1 (Fig. 1). Temperatures in ERA5 are higher than MERRA2 at the beginning of the satellite era, but converge over the past two decades (Supplementary Fig. 5).

When considered beside the apparent uniformity of trends in global temperature products, the differences between observational SST reconstructions present a conundrum. If one were to construct an ensemble of estimates of 60° S–60° N land and ocean temperatures using the four SST datasets and identical land temperature trends, one would expect the range in trends between these datasets to be ~0.74 × 0.076 (0.056) °C decade^{-1}. (The range in trends derived from the four SST datasets is 0.076 °C decade^{-1} and the ocean takes up 74% of the Earth's surface area between 60° S and 60° N.) However, the range in 60° S–60° N trends given by the five global temperature datasets is a mere 0.007 °C decade^{-1} (Fig. 2a). Why do the global temperature datasets exhibit such a small range of trends?

We separate the land and ocean components of global temperature datasets to calculate and compare their respective trends (Methods section on 'Processing'). Trends in SSTs from the ocean components of global temperature datasets are more similar to one another than SST trends from SST datasets (Fig. 2b,c). The range in SST trends from the global temperature datasets is 0.139–0.151 °C decade^{-1}, compared to 0.108–0.184 °C decade^{-1} in the SST datasets. SST trends from global temperature datasets fall in the middle of the range of those from the SST datasets. That is, none of the SST trends from global temperature datasets resembles those of the highest and lowest end-members of the SST datasets, HadISST1 and OISST v.2.1. We also note the slight apparent compensation between land and ocean temperature trends in the global temperature datasets, such that global temperature reconstructions

https://doi.org/10.1038/s41558-025-02362-6

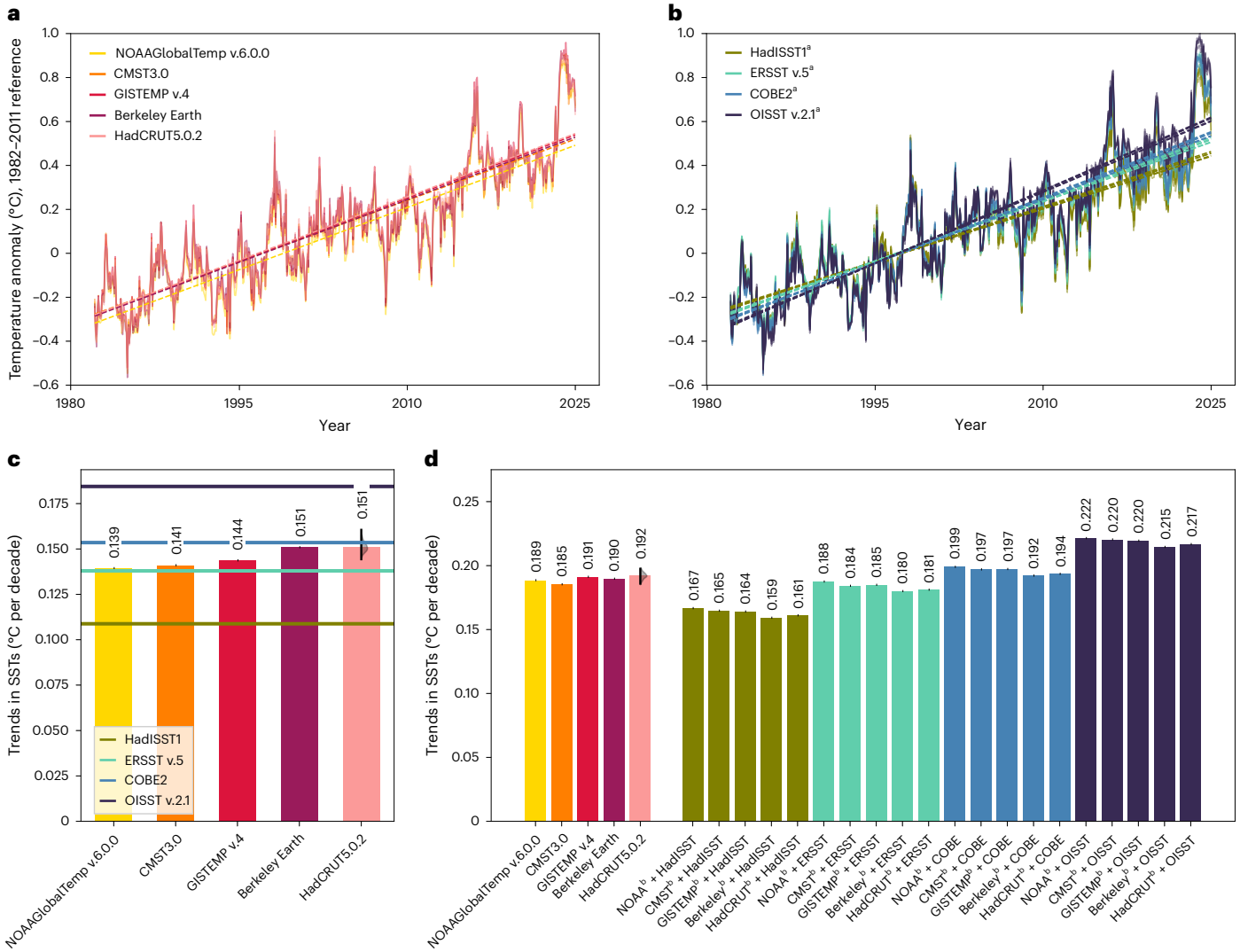

Fig. 2 | Comparing global to SST-only datasets. a, Time series of deseasonalized monthly average temperature anomalies, for all land and ocean between 60° S and 60° N. Data from the NOAAGlobalTemp v.6.0.0, CMST3.0, GISTEMP v.4, Berkeley Earth and HadCRTU5.0.2 datasets are shown in yellow, orange, red and pink, respectively. Temperature anomalies (°C) are against the 1982–2011 reference period. Dashed lines denote the linear trend between 1982 and 2024. **b**, Same as **a** but for temperature fields constructed from combinations of SSTs from each SST dataset and land temperatures from each global temperature dataset. A total of 20 time series with corresponding trend lines are shown, colour-coded by the SST field used. **c**, Trends in the ocean-only 60° S–60° N component of global temperature datasets, from 1982 to 2024 (n = 516 months), in °C per decade. The SST dataset trends corresponding to Fig. 1, on the right, are marked with horizontal coloured lines. The black error bar around the central estimate (ensemble mean) for HadCRUT5.0.2 spans the range of trends calculated from the 200-member ensemble, with kernel density estimates shaded in grey to indicate the distribution of ensemble trends. **d**, Trends in 60° S–60° N land and ocean temperature in the five global temperature datasets, and in each of these datasets if their SSTs were replaced with those from each of the four SST datasets, from 1982 to 2024 (n = 516 months). Error bars for HadCRUT5.0.2 similar to those in **c**, but for 60° S–60° N land and ocean temperature trends. [a]Plus land components from five global datasets. [b]Land component.

with relatively higher SST trends tend to have relatively lower land temperature trends and vice versa. The range of global temperature trends is smaller than the range of trends in the land or ocean components of these five datasets.

Combining SSTs from each SST-only dataset with land temperatures from each global temperature dataset (Methods section on 'Processing') yields a larger range of plausible global temperature trends than evident from global temperature datasets alone. The full ensemble of 60° S–60° N trends produced by all possible SST and land temperature combinations (Fig. 2d) spans from 0.159 °C decade^{-1} (Berkeley Earth land and HadISST) to 0.222 °C decade^{-1} (CMST land and OISST). The range in 60° S–60° N trends across all combinations of reconstructed SSTs and land temperature fields is thus an order of magnitude larger than the range given by global temperature datasets only (0.063 versus 0.007 °C decade^{-1}).

In published global temperature datasets, global average temperature anomalies and trends consistently fall within one another's estimated confidence intervals[9,11,13–15]. By contrast, the range of SST trends in the four SST products is larger than the ranges of trends derived from SST components of the uncertainty ensembles of global temperature datasets (Fig. 2c). Similarly, the range of plausible land and ocean temperature trends constructed using the four SST products is larger than the range derived from the reported uncertainty of global temperature datasets (Fig. 2d).

The SST reconstructions used in the five global temperature datasets are not independent: GISTEMP v.4, NOAAGlobalTemp v.6.0.0 and

https://doi.org/10.1038/s41558-025-02362-6

Table 1 | Dataset interdependency

Global temperature dataset	SST source	Land temperature source
GISTEMP v.4	ERSST v.5	GHCN v.4
HadCRUT v.5.0.2	HadSST4	CRUTEM5
NOAAGlobalTemp v.6.0.0	ERSST v.5	GHCN v.4
Berkeley Earth	HadSST4	Berkeley Earth monthly land temperature
CSMT3.0	ERSST v.5	C-LSAT2.1

Ocean and land temperature data sources for all-surface global temperature datasets.

CMST3.0 use ERSST v.5, while HadCRUT v.5.0.2 and Berkeley Earth use HadSST4 (Table 1 and Methods). SST trends in reanalysis are similarly dependent upon the choice of input dataset. MERRA2 reanalysis[16] uses OISST until March 2006, then the operational SST and sea-ice analysis (OSTIA)[17]. ERA5 (ref. 18) uses HadISST2.1.1.0 until August 2007, then OSTIA. Accordingly, MERRA2 exhibits a relatively high satellite-era trend of 0.176 °C decade^{-1}, while ERA5 exhibits a lower trend of 0.142 °C decade^{-1} (Fig. 1 and Supplementary Fig. 5).

Recent record warmth

The record-breaking global temperatures of 2023 and 2024, which coincided with devastating weather-related disasters in many parts of the world, motivated a proliferation of studies quantifying drivers of this 'spike' and situating it in the context of historical warming trends[19–25]. How anomalous were 2023 and 2024 in the satellite-era record? The answer is sensitive to dataset choice, as Fig. 3, which compares the SST datasets with the highest and lowest trend, demonstrates. The method of visualizing these data follows the 'climate reanalyzer' tool of the University of Maine, which uses OISST v.2.1 (ref. 26). In OISST v.2.1, average temperatures within the 1982–2011 reference period are 20.20 °C, with a standard deviation of 0.15 °C. Temperatures have exceeded the ±2 s.d. range from this reference period for most months in each year since 2014. In HadISST1, average temperatures in the reference period are 20.43 °C with a standard deviation of 0.11 °C, and only 7 years, including 2023–2024, exceed the ±2 s.d. range from the reference period.

In a steadily warming climate with natural variability, one should expect to see global temperature records broken somewhat regularly. Large year-on-year spikes in global mean temperature are most likely to coincide with El Niño events, especially those following long La Niña events[23]. Given these priors, how truly unprecedented were 2023–2024 temperature records? Record margins, which we compute as the difference between the monthly 60° S–60° N average SST and the previous record for that month since 1982, are largest during the 1997–1998, 2015–2016 and 2023–2024 El Niño events (Fig. 4). The relative magnitudes of these records are subject to observational uncertainty. In HadISST1, all monthly temperature record margins during the 2023–2024 El Niño are higher than those of the corresponding months of the 2015–2016 El Niño. The peak HadISST1 2023–2024 record margin, 0.28 °C in February 2024, exceeds the peak HadISST1 2015–2016 record margin of 0.15 °C in January 2016. In OISST, by contrast, the 2015–2016 El Niño event broke monthly global temperature records by comparable margins to the 2023–2024 El Niño event, although temperature record margins peaked relatively earlier during the 2023–2024 event. The OISST 2015–2016 maximum record margin of 0.30 °C in January 2016 just exceeds the OISST 2023–2024 record margin of 0.28 °C in August 2023.

Discussion

Interpretations that assume differences in trends between global temperature datasets to provide a reasonable estimate of true uncertainty are overconfident, as global temperature datasets do not account for the full range of trends in published SST reconstructions. As the IPCC (2021)[27] notes, global temperature reconstructions have 'far fewer methodological degrees of freedom than implied by a straight count of the number of available estimates'.

Systematic uncertainty—uncertainty due to, for example, the range of technical choices made by the different data-providing institutions—dwarfs parametric uncertainty in reconstructed SST and global temperature trends. Parametric uncertainty estimates, which sample known uncertainties introduced by measurement error, bias correction and aspects of the particular reconstruction methods used for each dataset[8,9,15] are small compared to interproduct differences. The statistical confidence interval measuring ±2 Newey–West standard errors, which conveys the scale of variability in the time-series data, is also small relative to the spread between datasets (Fig. 1).

The differences in satellite-era SST trends highlighted here are consequential. We suspect these differences are generally underappreciated, especially given that satellite measurements correct some known problems with presatellite-era temperature reconstructions[28]. Unless temperature records can be reconciled, the impact of SST trend uncertainties on the scientific literature must be evaluated. Below, we offer a non-exhaustive list of some implications of these uncertainties.

- *Global temperature extremes*. We considered the example of 2023–2024, the warmest two calendar years in the instrumental record (see 'Recent record warmth'). From a purely observational perspective, different SST reconstructions lend themselves to different views of the 2023–2024 warming spike. The 2023–2024 warming spike appears most anomalous in HadISST1, the SST dataset with the smallest trend (Fig. 3). In HadISST1, the record margins during the 2023–2024 El Niño are the largest in recent decades. In OISST v.2.1, the SST dataset with the largest trend, record margins during the 2023–2024 temperature spike are more similar to those during the 2015–2016 El Niño event (Fig. 4). Analyses of individual extreme years in the context of historical warming may be sensitive to systematic differences in reconstructed SST trends.
- *Transient climate response*. The transient climate response (TCR) of the Earth is the temperature change from doubling CO_2 following a 1% per year increase[29–31]. Following ref. 32, for a climate system with steadily increasing forcing from well-mixed greenhouse gases, the magnitude of climate change in response to a forcing F (units W m^{-2}) can be approximated by the heat balance $N = F - \alpha\Delta T$, where N (W m^{-2}) is the net heat flux into the system, α is a climate sensitivity parameter (W m^{-2} K^{-1}) and ΔT is the change in temperature. In approximation, $N = \kappa\Delta T$ where κ is an ocean heat uptake efficiency. Also $F = \rho\Delta T$ where $\rho \equiv \alpha + \kappa$. In the set of combinations of SST datasets and land components of global temperature datasets, including surface temperatures poleward of 30° S and 30° N from global temperature datasets, the combinations with the lowest and highest 1982–2024 trends are HadISST1 + CMST3.0 (0.166 °C decade^{-1}) and OISST v.2.1 + HadCRUT5.0.2 (0.237 °C decade^{-1}). Consulting the NOAA annual greenhouse gas index (https://gml.noaa.gov/aggi/aggi.html) for an estimate of historical radiative forcing, and assuming a radiative forcing from CO_2 doubling of 4.0 W m^{-2} (after ref. 30), yields TCR values of 1.79 and 2.55 °C corresponding to the HadISST1 + CMST3.0 and OISST v.2.1 + HadCRUT5.0.2 trends, respectively. This range represents uncertainty from satellite-era global temperature trend reconstruction, even if radiative forcing and the climate sensitivity parameter, which itself may be influenced by SST changes, were perfectly known.
- *SST-forced experiments*. Observational SST reconstructions are boundary conditions in atmospheric general circulation model (AGCM) experiments. Results in AGCM studies may be sensitive to the choice of SST dataset. For example, ref. 33 found that forcing an AGCM with HadISST1 versus Hurrell SSTs substantially impacted tropical atmospheric temperature trends. The standard tempera-

https://doi.org/10.1038/s41558-025-02362-6

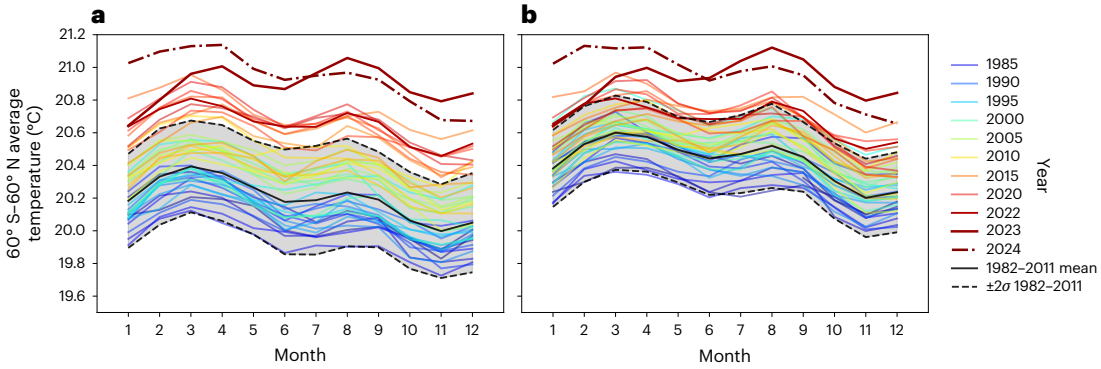

Fig. 3 | Choice of dataset impacts interpretation of warming trend and recent anomalies. Annual cycle of SST (°C) since 1982, with years coded by colour. The solid black line denotes the 1982–2011 monthly mean and the grey shaded area covers 2 s.d. from the reference period monthly mean. **a**,**b**, Contrast OISST v.2.1 (**a**) and HadISST1 (**b**).

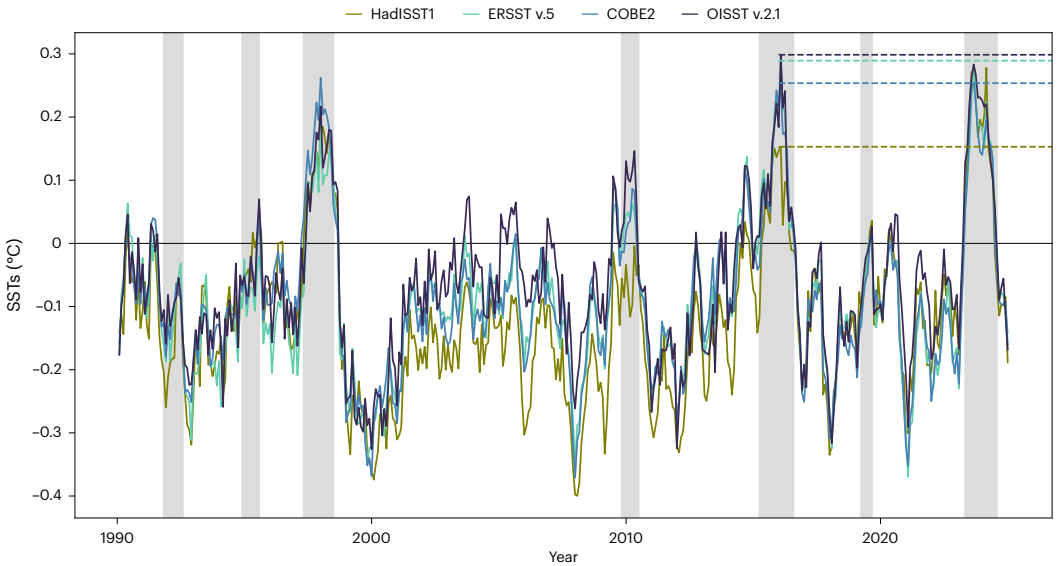

Fig. 4 | El Niño record margin unprecedented for HadISST, but comparable to 2015–2016 for ERSST, COBE and OISST. Time series of monthly record margins, that is the difference between the temperatures of the current month and the previous highest temperature since 1982, for 60° S–60° N average SSTs (°C) in four SST datasets. Values above zero are record-breaking monthly temperatures. Shaded in grey are El Niño events, defined here as periods during which the oceanic Niño index (3-month running mean) exceeds 0.5 °C for a minimum of five consecutive overlapping months. The dashed lines indicate the highest 2015–2016 El Niño record margins for comparison to recent records.

ture dataset used to force atmospheric model intercomparison project simulations is the merged Hadley-NOAA/OI sea surface temperature and sea-ice concentration dataset[34]. This dataset has a 1982–2021 (we use this range because more recent SSTs are not yet available at the time of writing) trend of 0.110 °C decade^{-1}, on the lower end of the four SST datasets' range in trends over that same time period (Supplementary Fig. 6; these trends are 0.093, 0.123, 0.143, 0.169 °C decade^{-1} for HadISST1, ERSST v.5, COBE2 and OISST v.2.1, respectively).

- *Radiative imbalance of Earth*. Quantifying the relationship between global temperatures and net top of atmosphere (TOA) radiative imbalances is important for understanding the drivers of global warming. While comparisons between climate models and observations of Earth's energy imbalance (EEI) indicate that the observed positive trend in EEI is highly unlikely to be a result of internal variability alone, both coupled and atmospheric climate models (AGCM) simulate trends in EEI at the lower end of the confidence interval derived from CERES observations[35]. Others[36] propose expanding such AGCM experiments to many models to intercompare simulated EEI trends, in part because revised SST estimates are available. Such analyses would be sensitive to the choice of SST dataset used, so should account for uncertainty across SST datasets. SST-forced AGCM experiments are also used in climate model development and evaluation to test the ability of models to reproduce the observed TOA energy imbalance; here, again, the choice of SST dataset matters, and may affect how coupled models ultimately simulate EEI trends.

Climate research centres devote substantial resources to the intercomparison of model simulations. Observations of air temperatures have also received much attention, leading to several revisions of key observational estimates such as the temperature measurements of the Microwave Sounding Unit[37–40]. By contrast, the systematic uncertainty across widely used SST datasets has not been adequately addressed. Credible estimates of the rate of satellite-era ocean warming diverge by several tenths of a °C per decade (Fig. 1). The agreement between global temperature datasets over the satellite era does not reflect the full range of plausible SST reconstructions, and consequently should

not be interpreted as a definitive measure of confidence in the rate of global warming.

We echo the recommendations of ref. 41, who stress the importance of maintaining thorough information about SST measurements, improving bias models and improving access to information. Making available the code used to produce SST reconstructions would better facilitate explorations of uncertainties within datasets and comparisons between datasets. We hope this analysis will help to inform data users of the systematic uncertainty in SST trends and to caution against using SST and global temperature data with undue assumptions of precisions.

Online content

Any methods, additional references, Nature Portfolio reporting summaries, source data, extended data, supplementary information, acknowledgements, peer review information; details of author contributions and competing interests; and statements of data and code availability are available at https://doi.org/10.1038/s41558-025-02362-6.

References

1. Freeman, E. et al. ICOADS Release 3.0: a major update to the historical marine climate record. *Int. J. Climatol.* **37**, 2211–2232 (2017).
2. Hausfather, Z. et al. Assessing recent warming using instrumentally homogeneous sea surface temperature records. *Sci. Adv.* **3**, e1601207 (2017).
3. Rayner, N. A. Global analyses of sea surface temperature, sea ice, and night marine air temperature since the late nineteenth century. *J. Geophys. Res.* **108**, 4407 (2003).
4. Huang, B. et al. Extended reconstructed sea surface temperature, version 5 (ERSSTv5): upgrades, validations, and intercomparisons. *J. Clim.* **30**, 8179–8205 (2017).
5. Huang, B. et al. Improvements of the daily optimum interpolation sea surface temperature (DOISST) version 2.1. *J. Clim.* **34**, 2923–2939 (2021).
6. Hirahara, S., Ishii, M. & Fukuda, Y. Centennial-scale sea surface temperature analysis and its uncertainty. *J. Clim.* **27**, 57–75 (2014).
7. Hansen, J., Ruedy, R., Sato, M. & Lo, K. Global surface temperature change. *Rev. Geophys.* https://doi.org/10.1029/2010RG000345 (2010).
8. Lenssen, N. J. L. et al. Improvements in the GISTEMP uncertainty model. *J. Geophys. Res. Atmos.* **124**, 6307–6326 (2019).
9. Morice, C. P. et al. An updated assessment of near-surface temperature change from 1850: the HadCRUT5 data set. *J. Geophys. Res.: Atmos.* **126**, e2019JD032361 (2021).
10. Yin, X. et al. NOAAGlobalTemp version 6: an AI-based global surface temperature dataset. *Bull. Am. Meteorol. Soc.* **105**, E2184–E2193 (2024).
11. Rohde, R. A. & Hausfather, Z. The Berkeley Earth land/ocean temperature record. *Earth Syst. Sci. Data* **12**, 3469–3479 (2020).
12. Sun, W. et al. Description of the China global merged surface temperature version 2.0. *Earth Syst. Sci. Data* **14**, 1677–1693 (2022).
13. Huang, B. et al. Uncertainty estimates for sea surface temperature and land surface air temperature in NOAAGlobalTemp version 5. *J. Clim.* **33**, 1351–1379 (2020).
14. Jones, P. The reliability of global and hemispheric surface temperature records. *Adv. Atmos. Sci.* **33**, 269–282 (2016).
15. Lenssen, N. et al. A NASA GISTEMPv4 observational uncertainty ensemble. *JGR Atmos.* **129**, e2023JD040179 (2024).
16. Gelaro, R. et al. The modern-era retrospective analysis for research and applications, version 2 (MERRA-2). *J. Clim.* **30**, 5419–5454 (2017).
17. Donlon, C. J. et al. The operational sea surface temperature and sea ice analysis (OSTIA) system. *Remote Sens. Environ.* **116**, 140–158 (2012).
18. Hersbach, H. et al. The ERA5 global reanalysis. *Q. J. R. Meteorol. Soc.* **146**, 1999–2049 (2020).
19. Rantanen, M. & Laaksonen, A. The jump in global temperatures in September 2023 is extremely unlikely due to internal climate variability alone. *Npj Clim. Atmos. Sci.* **7**, 1 (2024).
20. Cheng, L. et al. New record ocean temperatures and related climate indicators in 2023. *Adv. Atmos. Sci.* **41**, 1068–1082 (2024).
21. Esper, J., Torbenson, M. & Büntgen, U. 2023 summer warmth unparalleled over the past 2,000 years. *Nature* **631**, 94–97 (2024).
22. Li, K. et al. El Niño and the AMO sparked the astonishingly large margin of warming in the global mean surface temperature in 2023. *Adv. Atmos. Sci.* **41**, 1017–1022 (2024).
23. Raghuraman, S. P. et al. The 2023 global warming spike was driven by the El Niño–Southern Oscillation. *Atmos. Chem. Phys.* **24**, 11275–11283 (2024).
24. Beaulieu, C. et al. A recent surge in global warming is not detectable yet. *Commun. Earth Environ.* **5**, 576 (2024).
25. Terhaar, J. et al. Record sea surface temperature jump in 2023–2024 unlikely but not unexpected. *Nature* **639**, 942–946 (2025).
26. Climate Reanalyzer (n.d.). 'Daily Sea Surface Temperature' (Climate Change Institute, accessed 30 November 2023); https://climatereanalyzer.org/
27. *Climate Change 2021: The Physical Science Basis*. Contribution of Working Group I to the Sixth Assessment Report of the Intergovernmental Panel on Climate Change (IPCC, 2021); https://www.ipcc.ch/report/ar6/wg1/
28. Chan, D. & Huybers, P. Systematic differences in bucket sea surface temperatures caused by misclassification of engine room intake measurements. *J. Clim.* **33**, 7735–7753 (2020).
29. Gillett, N. P., Arora, V. K., Flato, G. M., Scinocca, J. F. & von Salzen, K. Improved constraints on 21st-century warming derived using 160 years of temperature observations. *Geophys. Res. Lett.* https://doi.org/10.1029/2011GL050226 (2012).
30. Sherwood, S. C. et al. An assessment of Earth's climate sensitivity using multiple lines of evidence. *Rev. Geophys.* **58**, e2019RG000678 (2020).
31. Morgenstern, O. Using historical temperature to constrain the climate sensitivity, the transient climate response, and aerosol-induced cooling. *Atmos. Chem. Phys.* **24**, 8105–8123 (2024).
32. Gregory, J. M. & Forster, P. M. Transient climate response estimated from radiative forcing and observed temperature change. *J. Geophys. Res. Atmos.* https://doi.org/10.1029/2008JD010405 (2008).
33. Flannaghan, T. J. et al. Tropical temperature trends in Atmospheric General Circulation Model simulations and the impact of uncertainties in observed SSTs. *J. Geophys. Res. Atmos.* https://doi.org/10.1002/2014JD022365 (2014).
34. Hurrell, J. W., Hack, J. J., Shea, D., Caron, J. M. & Rosinski, J. A new sea surface temperature and sea ice boundary dataset for the community atmosphere model. *J. Clim.* **21**, 5145–5153 (2008).
35. Raghuraman, S. P., Paynter, D. & Ramaswamy, V. Anthropogenic forcing and response yield observed positive trend in Earth's energy imbalance. *Nat. Commun.* **12**, 4577 (2021).
36. Schmidt, G.A. et al. CERESMIP: a climate modeling protocol to investigate recent trends in the Earth's Energy Imbalance. *Front. Clim.* https://doi.org/10.3389/fclim.2023.1202161 (2023).
37. Christy, J. R., Spencer, R. W. & Braswell, W. D. MSU tropospheric temperatures: dataset construction and radiosonde Comparisons. *J. Atmos. Ocean. Technol.* **17**, 1153–1170 (2000).
38. Thorne, P. W., Lanzante, J. R., Peterson, T. C., Seidel, D. J. & Shine, K. P. Tropospheric temperature trends: history of an ongoing controversy. *WIREs Clim. Change* **2**, 66–88 (2011).

39. Po-Chedley, S. & Fu, Q. Discrepancies in tropical upper tropospheric warming between atmospheric circulation models and satellites. *Environ. Res. Lett.* **7**, 044018 (2012).
40. Po-Chedley, S., Thorsen, T. J. & Fu, Q. Removing diurnal cycle contamination in satellite-derived tropospheric temperatures: understanding tropical tropospheric trend discrepancies. *J. Clim.* **28**, 2274–2290 (2015).
41. Kent, E. C. et al. A call for new approaches to quantifying biases in observations of sea surface temperature. *Bull. Am. Meteorol. Soc.* **98**, 1601–1616 (2017).

https://doi.org/10.1038/s41558-025-02362-6

Methods

Sea surface temperature datasets

We compare four spatially infilled and regularly updated SST products. We use the most current version of each dataset as of the time of writing. Here we provide brief descriptions of each dataset with references to detailed information.

HadISST1. HadISST1 (ref. 3) provides SSTs and sea-ice concentration on a 1° × 1° latitude–longitude grid beginning in 1870. SST input data include in situ observations from the Met Office Marine Data Bank and ICOADS and satellite-based observations from advanced very high-resolution radiometer (AVHRR) sensors. The SST reconstruction method uses reduced-space optimal interpolation, with additional measures taken to account for long-term SST changes since the late nineteenth century. Gridded observations are re-introduced to restore variance on ~500-km scales. Both in situ and satellite observations are used from 1982 onwards. SSTs near sea ice are estimated using statistical relationships between SST and sea-ice concentration. Unlike ERSST v.5, COBE2 and OISST v2.1, no SSTs are given for sea-ice areas. HadISST1 data may be accessed at https://hadleyserver.metoffice.gov.uk/hadisst/data/download.html.

ERSST v.5. ERSST v.5 (ref. 4) is produced by NOAA and provides SST data on a 2° × 2° latitude–longitude resolution from 1854 to the present. SST input data are primarily from ICOADS and Argo data above 5 m. SST data are quality controlled and adjusted for mutual consistency. SST observations are separated into low- and high-frequency components, and high-frequency components are reconstructed using empirical orthogonal teleconnections. SSTs near sea ice are relaxed towards a representative freezing temperature of seawater (−1.8 °C) based on sea-ice concentration. Uncertainties for ERSST v.4, which used similar methods to ERSST v.5, are described by ref. 42. ERSST v.5 data are available at https://www.ncei.noaa.gov/access/metadata/landing-page/bin/iso?id=gov.noaa.ncdc:C00927.

COBE2. COBE2 (ref. 6) is a product of the JMA and provides SST data from 1850 to the present on a 1° × 1° latitude–longitude grid. SST input data include ICOADS release 2.5 and additional SST data compiled by the JMA, plus AVHRR data to reconstruct variability in data-sparse regions. An empirical orthogonal function-based method is used to reconstruct SSTs. In areas with sea ice, SSTs are computed on the basis of sea-ice concentration such that areas around sea ice are close to the climatological salinity-dependent freezing point of seawater. COBE2 data are accessible from https://psl.noaa.gov/data/gridded/data.cobe2.html.

OISST v.2.1. OISST v.2.1 (ref. 5) from NOAA provides a record of SSTs beginning in September 1981 at 0.25° latitude–longitude resolution. SST input data are from AVHRR and ICOADS3.0. After adjusting ship SSTs for biases and adjusting AVHRR measurements to match in situ SSTs at 0.2-m depth, the input data are combined using optimum interpolation. When sea-ice concentrations are >35%, SSTs are replaced by the climatological salinity-dependent freezing point of seawater. Daily OISST v.2.1 data are available at https://www.ncei.noaa.gov/data/sea-surface-temperature-optimum-interpolation/v2.1/access/avhrr/.

Global temperature datasets

We consider four publicly available and regularly updated global (land and ocean) surface temperature products, taking the most current version of each dataset as of the time of writing. These global temperature datasets combine SSTs with near-surface (~2 m) land temperatures.

GISTEMP v.4. GISTEMP v.4 (refs. 7,8) provides global temperatures on a 2 × 2 grid from 1880 to the present. The input data are ERSST v.5 for SSTs and NOAA global historical climatology network version 4 (GHCN v.4) for land surface air temperatures. Others[8] calculate uncertainties in GISTEMP global and annual mean temperature anomalies by combining the ERSST v.4 uncertainty analysis from ref. 42, which considers empirical orthogonal teleconnection function reconstruction uncertainties and parametric uncertainties and land temperature uncertainties from sampling and homogenization. GISTEMP data are available at https://data.giss.nasa.gov/gistemp/.

HadCRUT v.5.0.2. HadCRUT5 (ref. 9) is a 5° latitude–longitude global temperature dataset spanning from 1850 to the present. Input data are the UK Met Office Hadley Centre SST dataset (HadSST4)[43] for SSTs and Climatic Research Unit temperature version 5 (CRUTEM5)[44] for surface air temperatures. The central estimate is the average of a 200-member ensemble. The ensemble members are intended to sample the distribution of systematic observational uncertainties and uncertainties in the analysis of observations. The ensemble members were not used in the final version of this analysis because they are not yet available through 2024. The infilled 'HadCRUT5 analysis' ensemble members and ensemble mean are available for download at https://www.metoffice.gov.uk/hadobs/hadcrut5/data/HadCRUT.5.0.2.0/download.html.

NOAAGlobalTemp v.6.0.0. NOAAGlobalTemp[45] is provided on a 5° × 5° latitude–longitude grid from 1850 to the present. Input data are ERSST v.5 for SSTs and GHCN v.4 for land surface air temperatures. Version 6.0.0 uses an artificial neural network method to improve reconstruction of land surface temperatures. Uncertainties at global and local scales are described for NOAAGlobalTemp version 5 (ref. 13), but have not yet been estimated for version 6. NOAAGlobalTempv6.0.0 data are available at https://www.ncei.noaa.gov/data/noaa-global-surface-temperature/v6/access/gridded/.

Berkeley Earth. The Berkeley Earth global temperature dataset[11] is provided on a 1° × 1° latitude–longitude grid from 1850 to the present. Input data are HadSST4 for SSTs (personal communication, Z. Hausfather) and the Berkeley Earth monthly land temperature dataset for land surface air temperatures. Berkeley Earth uncertainty estimates[11] combine measurement and sampling uncertainty, coverage uncertainty and bias uncertainty. Berkeley Earth global gridded data on a 1 × 1 latitude–longitude grid are available at https://berkeleyearth.org/data/.

CMST3.0. CMST3.0 (ref. 12) dataset is provided on a 5° × 5° latitude–longitude grid from 1850 to the present. Input data are ERSST v.5 for SSTs and the China-land surface air temperature version 2.1 product for land temperatures (C-LSAT2.1)[46]. C-LSAT2.1 integrates 14 data sources (three global, three regional and eight national) for maximum spatial coverage over land. CMST3.0 data are accessible at http://www.gwpu.net/en/h-col-103.html; we use the 'China-MST3.0 Nrec' data product.

Processing

We analyse latitudes from 60° S to 60° N. We focus on this area because some reconstructions report the temperature of the sea surface directly under ice, while others report near-surface air temperatures over ice. Excluding polar regions, which comprise 14% of the surface area of the Earth, permits us to compare these datasets directly. If polar regions were included, the choice of how to treat sea ice could significantly impact global mean temperatures[11].

Deseasonalized monthly average data are produced by subtracting the monthly climatology from the temperature each month, then adding the difference to the climatological average. Using annual mean temperatures instead of deseasonalized monthly data would have little effect on the results of this study.

Decadal temperature trends were calculated using ordinary least squares regression. Because the time-series data are autocorrelated, we use the Newey–West estimator[47] to produce the ±2 standard error range

reported in Fig. 1. The maximum lag considered in the autocorrelation structure is 5 months. Although the values of temperature trends in a period of this duration (43 years) are sensitive to small shifts in start and end dates, the overall results of this analysis are not.

Global temperature datasets were split into land and ocean components to calculate respective trends. We used the land/sea masks or land fraction weights provided by each group. For CMST3.0, we used the HadCRUT5.0.2 land weights because the two datasets use the same 5 × 5 grid. Grid points were considered 'land' where the land fraction >0.5. Grid points were considered 'ocean' where the land fraction was ≤0.5.

For each combination of SST data and land component of global temperature data used to calculate the trends in Fig. 2, the SST data were first regridded to the latitude/longitude grid of the global temperature dataset. The land component of the global temperature dataset was combined with the regridded SSTs. Any remaining grid cells were filled using linear interpolation in space. Finally, trends were calculated from deseasonalized monthly means.

Data availability

All data used for this analysis are publicly available. SST datasets include HadISST1 (https://hadleyserver.metoffice.gov.uk/hadisst/data/download.html), ERSST v.5 (https://www.ncei.noaa.gov/access/metadata/landing-page/bin/iso?id=gov.noaa.ncdc:C00927), COBE2 (https://psl.noaa.gov/data/gridded/data.cobe2.html) and OISST v.2.1 (https://www.ncei.noaa.gov/data/sea-surface-temperature-optimum-interpolation/v2.1/access/avhrr/). Global temperature datasets include GISTEMP v.4 (https://data.giss.nasa.gov/gistemp/), HadCRUT v.5.0.2 (https://www.metoffice.gov.uk/hadobs/hadcrut5/data/HadCRUT.5.0.2.0/download.html), NOAAGlobalTemp v.6.0.0 (https://www.ncei.noaa.gov/data/noaa-global-surface-temperature/v6/access/gridded/), Berkeley Earth (https://berkeleyearth.org/data/) and CMST3.0 (http://www.gwpu.net/en/h-col-103.html). Reanalysis data include ERA5 (https://www.ecmwf.int/en/forecasts/dataset/ecmwf-reanalysis-v5) and MERRA2 (https://gmao.gsfc.nasa.gov/reanalysis/merra-2/data_access/). Data to reproduce the figures in this analysis are available via Princeton University at https://doi.org/10.34770/v1rs-gq54 (ref. 48).

Code availability

Code to reproduce the figures in this analysis are available via Princeton University at https://doi.org/10.34770/v1rs-gq54 (ref. 48).

References

42. Huang, B. et al. Further exploring and quantifying uncertainties for extended reconstructed sea surface temperature (ERSST) version 4 (v4). *J. Clim.* **29**, 3119–3142 (2016).
43. Kennedy, J. J., Rayner, N. A., Atkinson, C. P. & Killick, R. E. An ensemble data set of sea surface temperature change from 1850: the Met Office Hadley Centre HadSST.4.0.0.0 data set. *J. Geophys. Res. Atmos.* **124**, 7719–7763 (2019).
44. Osborn, T. J. et al. Land surface air temperature variations across the globe updated to 2019: the CRUTEM5 data set. *J. Geophys. Res. Atmos.* **126**, e2019JD032352 (2021).
45. Huang, B., Yin, X., Menne, M. J., Vose, R. & Zhang, H.-M. Improvements to the land surface air temperature reconstruction in NOAAGlobalTemp: an artificial neural network approach. *Artif. Intell. Earth Syst.* https://doi.org/10.1175/AIES-D-22-0032.1 (2022).
46. Xu, Q., Wei, S., Li, Z. & Li, Q. A new evaluation of observed changes in diurnal temperature range. *Geophys. Res. Lett.* **52**, e2024GL113406 (2025).
47. Newey, W. K. & West, K. D. Hypothesis testing with efficient method of moments estimation. *Int. Econ. Rev.* **28**, 777–787 (1987).
48. Menemenlis, S. Data and code for figures in 'Consequential differences in satellite-era sea surface temperature trends across datasets' [Dataset]. *Princeton University* https://doi.org/10.34770/v1rs-gq54 (2025).

Acknowledgements

We acknowledge and thank the groups that produced the reconstructions of SSTs and global temperatures used in this article. This work was supported in part by NASA grant no. 80NSSC22K0999 21-OSST21-0016 (G.A.V., W.Y. and S.M.), Heising-Simons Foundation Award no. 2023-4721 (G.A.V. and W.Y.) and USDOC-NOAA grant no. 2018NA18OAR4320123 (S.M.). We thank M. Chung, H. He and C. Beaulieu for helpful conversations about previous drafts of this manuscript.

Author contributions

All authors contributed conceptual and technical input. S.M. analysed the data and wrote the manuscript and all authors contributed to editing.

Competing interests

The authors declare no competing interests.

Additional information

Supplementary information The online version contains supplementary material available at https://doi.org/10.1038/s41558-025-02362-6.

Correspondence and requests for materials should be addressed to S. Menemenlis.

Peer review information *Nature Climate Change* thanks the anonymous reviewers for their contribution to the peer review of this work.